

23

**И Н С Т И Т У Т
ЯДЕРНОЙ ФИЗИКИ СОАН СССР**

ПРЕПРИНТ И Я Ф 60 - 73

Yu.I.Abrashitov, V.V.Konyukhov, V.S.Koydan, V.M.Lagunov,
V.N.Tukyanov, K.I.Mekler, D.D.Ryutov

INTERACTION OF A HIGH-POWER RELATIVISTIC ELECTRON
BEAM WITH A PLASMA IN A MAGNETIC FIELD

Новосибирск

1973

I. Introduction

First experiments on the interaction of a high-power relativistic electron beam with a plasma were carried out in 1970-1971 at the Novosibirsk Institute of Nuclear Physics [1]. In these experiments, a beam with electron energy $E_b = 2 \div 3$ MeV and density $n_b = 5 \cdot 10^{10} \text{ cm}^{-3}$ was injected along a magnetic field $H = 1 \div 2$ kOe into a plasma with density $n = 10^{11} \div 10^{14} \text{ cm}^{-3}$. It was found out that under some conditions the beam delivered to the plasma a noticeable fraction*) ($\sim 10\%$) of its initial energy. This fact can be explained only by collective effects, because in the experiment [1] the Coulomb mean free paths of both the plasma and beam electrons were much greater than the length of the machine. Thus, the existence of the effective collective interaction of a high-current relativistic electron beam with a plasma was first demonstrated in paper [1].

In the experiment [1] the energy delivered by the beam to plasma depended substantially on the plasma density. The energy was maximum at $n \sim 10^{12} \text{ cm}^{-3}$ and fell down rapidly both at a decrease and (what is more essential) at an increase of the plasma density. Theory [1,2] shows that in order to increase an effectiveness of a plasma heating in a high-density region one should increase a density of the beam particles n_b , decrease their ener-

*) This quantity is not given in the paper [1] in a direct form. Our estimate is based on the results of diamagnetic measurements published in [1].

gy E_b , and increase a longitudinal magnetic field H . In accordance with these indications of theory, an installation "INAR" [3] was built at the Novosibirsk Institute of Nuclear Physics. Its parameters are as follows: beam density n_b up to $5 \cdot 10^{11} \text{ cm}^{-3}$; beam energy $E_b = 1 \text{ MeV}$; longitudinal magnetic field H up to 15 kOe .

In what follows, the physical results obtained at the "INAR" installation are communicated.

2. Experimental Setup and Diagnostics

The diagram of the setup is shown in Fig. I. Electron beam with initial energy 1 MeV , current 5 kA , and duration $50\text{--}70 \text{ nsec}$ was generated by a pulsed electron accelerator. The energy store I (which was a cylindrical condenser with capacity 500 pF) was charged to the voltage 1.5 MV by means of a pulses transformer. When the voltage at the store reached a maximum, then the gaseous spark-gap 2 was switched and the voltage was supplied to the vacuum diode 4. A hollow 2 cm -diameter stainless steel cylinder with thin walls and flat base was used as a field-emission cathode.

The main part of the vacuum chamber (6) was a 220 cm -long glass tube with inner diameter 11 cm . It was connected with the accelerator by means of a cylindrical stainless steel transition with wall thickness 1 mm . The vacuum chamber was limited at both ends by two titanium foils, each 50μ thick, one of these foils being an anode of the accelerator. A beam current, passing through a vacuum tube, was received by an end electrode (II). This electrode was connected with the accelerator by four

return current conductors (8) placed at the outer surface of the vacuum chamber.

Quasistationary magnetic field of a mirror configuration (mirror ratio 1,7) was created by the coil (10) with inner

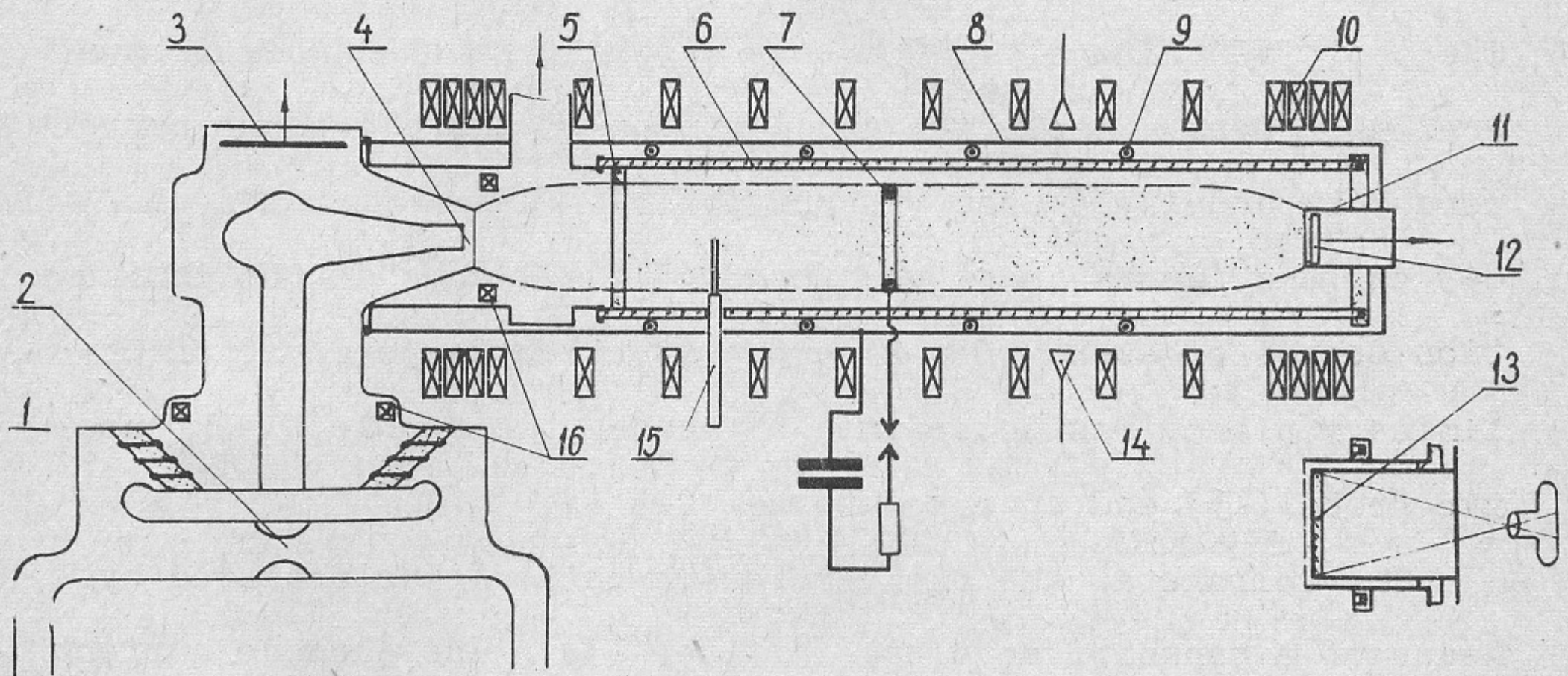


Fig.1. Diagram of setup: 1-energy store, 2-spark-gap, 3-capacitive voltage divider, 4-field-emission diode, 5-quartz diaphragm, 6-vacuum chamber, 7-anode of Penning discharge, 8-return current conductors, 9-diamagnetic probes, 10-coil of quasistationary magnetic field, 11-beam collector, 12-calorimeter and shunt, 13-plasmoscope, 14-microwave horns, 15-double electrostatic probe, 16-Rogovski coils.

diameter 20 cm. The distance between mirrors was 230 cm. The maximum value of the magnetic field in the centre of the machine was 15 kOe, inhomogeneities in this region being less than 1 per cent.

Preliminary plasma was created by a pulsed Penning-type discharge. The end foils (which were located in the mirrors) were used as cathodes of the discharge. An 8 cm - diameter ring (7) placed in the middle of the vacuum chamber was used as an anode. The positive voltage ~ 20 kV was supplied to the anode from a condenser bank. Amplitude and duration of the discharge current were 5 kA and $10\div 15$ μ sec, respectively. Plasma diameter was $8\div 9$ cm, and plasma density reached $(3\div 4)\cdot 10^{14}$ cm^{-3} at the ionization degree of about 50 per cent. Electron temperature of preliminary plasma was determined by means of a double electrostatic probe (15) and appeared to be $2\div 3$ eV.

The voltage at the field-emission cathode was measured by means of a capacitive voltage divider (3). The cathode current and the total current in plasma were measured with Rogovski coils (16). The beam current at the end of the vacuum chamber and the total energy transported by the beam, were measured with shunt and with graphite calorimeter*), respectively. They were mounted together in a single device (12). In some experiments thin plastic**) plates were placed behind the exit foil in order to register the shape of the beam cross-section. The darkening of these plates is a measure of the number of electrons striking the plate^[4].

*) Note that the diameter of the calorimeter (6cm) was considerably greater than the diameter of the beam, passing through the machine in a vacuum (2,5 cm).

**) In particular, astralon.

The plasma density was determined from the cut-off measurements at the wave-lengths 2,4,8,13,30 mm, and also by means of a microwave interferometer at $\lambda = 8$ mm. The density distribution in the plane, perpendicular to the magnetic field, was determined by means of a plasmoscope (13) of a described in Ref. [5] type.

Perpendicular plasma pressure was registered with four single-turn diamagnetic probes (9), each 13 cm in diameter. They were placed under the return current conductors at distances 35, 90, 140, 190 cm from the left mirror. The probes were loaded with the integrating circuits with time-constant $RC \cong 1$ μ sec. Diamagnetic signals were registered at oscilloscopes with bandwidth 60 MHz. The time resolution of the diamagnetic probes was better than 10 nsec.

3. Propagation of the Beam through the Vacuum

When the beam is injected into a vacuum (background pressure 10^{-6} torr), then the total beam energy Q , transmitted through the tube, and the amplitude of the exit current I_{exit} strongly depends on the magnetic field intensity H . At $H=0$ the current and the energy transmitted through the tube are zero, that is, the beam does not pass through the tube. It is evident that the beam is destroyed at the beginning of its way in a vacuum. In the region of weak magnetic fields, Q and I_{exit} grow monotonically with H , but after some critical value of H ($H_{\text{crit}} \cong 5$ kOe) they become independent of H . The $Q(H)$ dependence is shown in Fig.2. At the initial energy of the beam $E_0 = 1$ MeV and $H > 5$ kOe the average

value of Q is 70 J, and the amplitude of I_{exit} is approximately equal to 3 kA. It is reasonable to compare the last quantity with the theoretical value of the critical current. Elementary calculations (see [6]) show that in the case of a cylindrical return current conductor, with radius R considerable exceeding the beam radius r_b , the critical current is determined by the formula *)

$$I_{\text{crit}} = \frac{mc^3}{e} \frac{(\gamma_0^{2/3} - 1)^{3/2}}{1 + 2 \ln \frac{R}{r_b}} \quad (1)$$

where $\gamma_0 = 1 + \frac{E_0}{mc^2}$, E_0 being the initial kinetic energy of the beam. With $\gamma_0 = 3$ and $\ln \frac{R}{r_b} = 2$ one gets from (1) $I_{\text{crit}} \cong 4$ kA, this value being a little greater than the observed limiting current **). This (small) discrepancy can be explained partly by the influence of an inductive electric field which is due to the unstationary character of the beam and partly by the reduction of a longitudinal momentum of the beam electrons due to the scattering in the entrance foil (an angular spread $\sqrt{\theta_0^2}$ of 1 MeV electrons in a 50μ titanium foil is equal to $15-20^\circ$)

*) In our case the return current conductor was done in a form of four rods parallel to the axis of the system, but the allowance for that fact gives rise only to a small correction ($\sim (r_b/R)^4$) to formula (1). Note that this formula itself has the accuracy $\sim (2 \ln R/r_b)^{-1}$

**.) Note that the injected current was equal to 5÷6 kA (this follows from the experiments on the beam injection into a dense plasma, see Sec.4 of the present article), In a vacuum some fraction of this current returned to the accelerator. The reflection took place at a distance of the order of several R 's from the entrance foil.

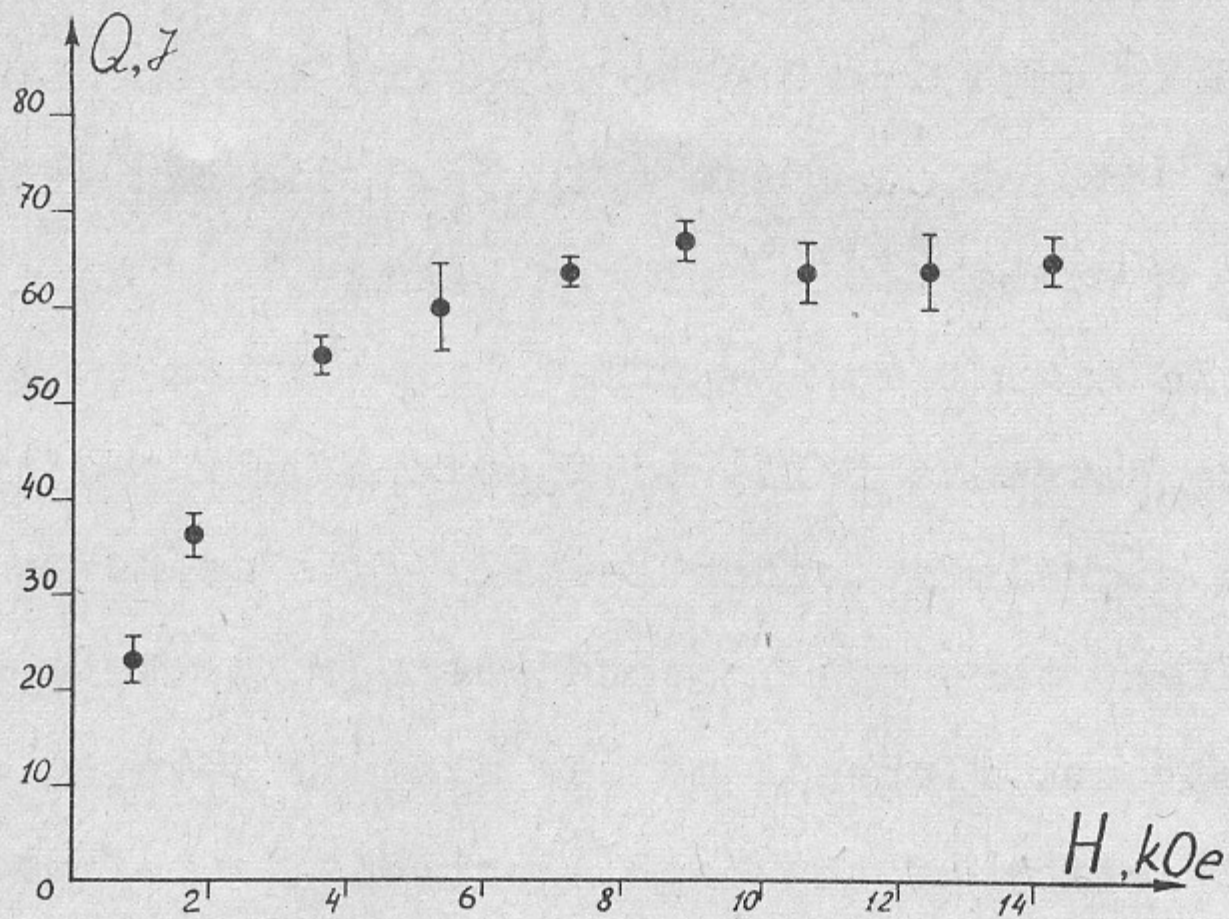


Fig.2. The magnetic field dependence of energy transmitted by the beam through the vacuum.

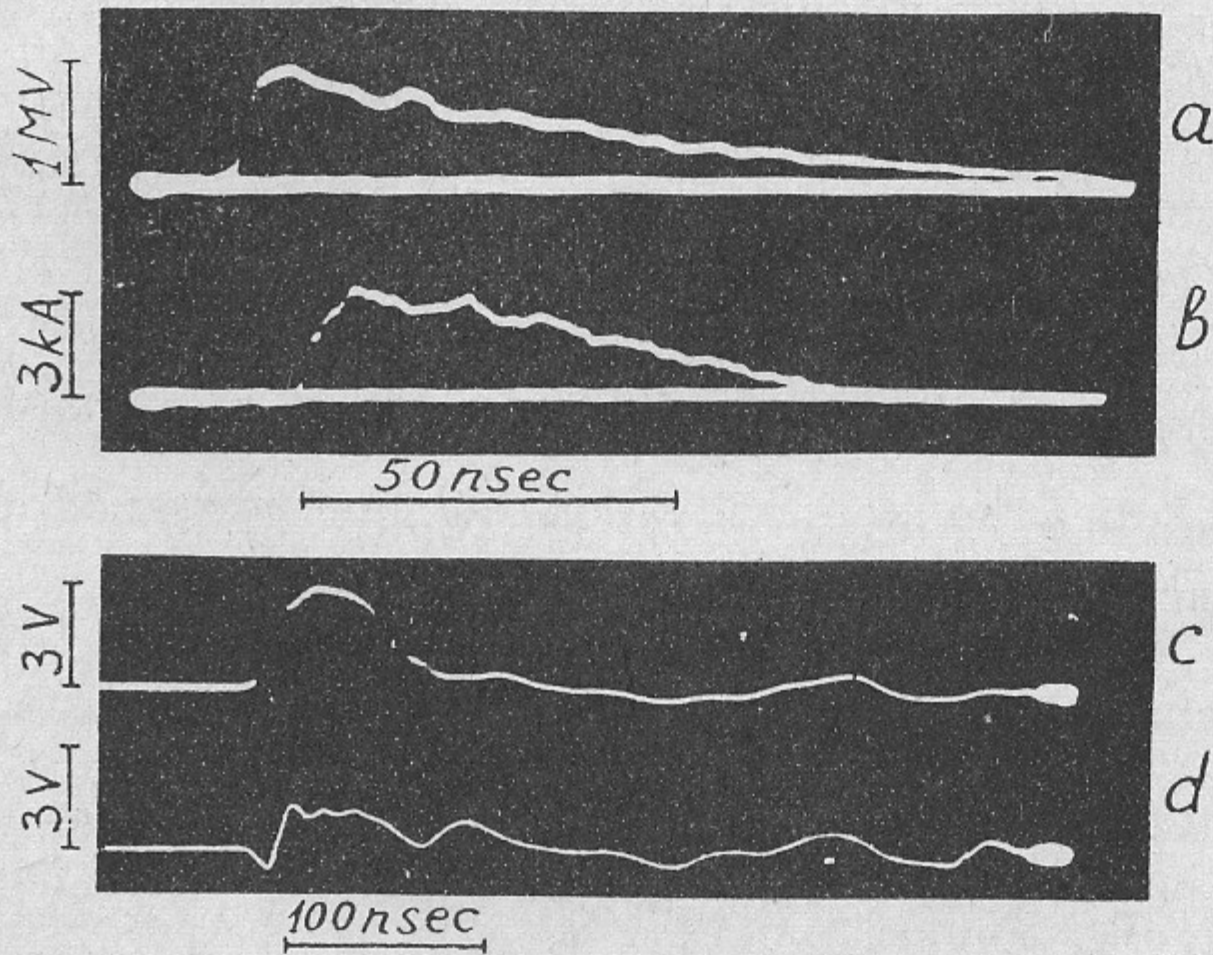


Fig.3. The typical oscillograms (vacuum, $H=7$ kOe):
 a-voltage at the field-emission cathode; b-exit current of the beam; the delay time of the exit current is with reasonable accuracy equal to L/c ;
 c,d-integrated signals from the first and the second diamagnetic probes (1 Volt correspond to $W=5 \cdot 10^{16}$ eV.cm⁻¹ at $H=7$ kOe).

When the beam passes through vacuum, then diamagnetic probes record some signals with 15-20 nsec risetime and duration approximately equal to that of the beam (Fig.3). One can interpret these signals as a diamagnetism of the beam.

The diamagnetic signal at the first loop (which is at 35 cm distance from the entrance foil) is approximately two times greater than the signals at other loops. This seems to be connected with the fact that the injected beam current is higher than the critical one. Indeed, as was already pointed out, in this case some fraction of the beam electrons is reflected backward, and the diamagnetisms of the forward and backward currents are summed.

Diamagnetism of a beam in a vacuum is determined by two effects. The first is the existence of perpendicular momenta of the beam electrons (the corresponding contribution to the perpendicular pressure being $\mathcal{P}'_1 = \frac{1}{2} n_b \overline{p_1 v_1} = \frac{n_b}{2} \frac{p_1^2}{m\gamma}$). The second is the electrostatic repulsion of the beam, partly compensated by magnetic contraction (the contribution to the perpendicular pressure being $\mathcal{P}''_1 = \frac{5}{2} \frac{r^2 e^2 n_b^2}{\gamma^2}$). Taking into account the conservation of an adiabatic invariant $p_1^2/H = \text{const}$, one can write that

$$\mathcal{P}'_1 = \frac{n_b}{2} \frac{\overline{p_{10}^2}}{m\kappa\gamma} = \frac{n_b p_0^2 \overline{\theta_0^2}}{2m\kappa\gamma} = n_b mc^2 \frac{(\gamma_0^2 - 1) \overline{\theta_0^2}}{2\gamma\kappa},$$

where κ is the mirror ratio, and subscript "0" denotes the initial values of the corresponding quantities (in the mirror).

Generally speaking, the value of γ inside a machine differs from γ_0 (due to electrostatic retardation of the beam). In

our experiments the beam current was close enough to the critical one. As one can see, relationship $\gamma = \gamma_0^{1/3}$ holds in this case. Hence,

$$P_1' = n_b mc^2 \frac{(\gamma_0^2 - 1) \overline{\theta_0^2}}{2 \gamma_0^{1/3} \kappa}$$

The quantity which is determined from the diamagnetic measurements is

$$W_1 = 2\pi \int (P_1' + P_1'') r dr \equiv W_1' + W_1''$$

(W_1 being directly related to the magnetic flux variation $\Delta\Phi$, $W_1 = H \Delta\Phi / 4\pi$). One can express W_1' and W_1'' in terms of a beam current:

$$W_1' = \frac{mc I_b}{e} \frac{\gamma_0^2 - 1}{\sqrt{\gamma_0^{2/3} - 1}} \frac{\overline{\theta_0^2}}{2\kappa} \quad (2)$$

$$W_1'' = \frac{I_b^2}{2c^2(\gamma_0^{2/3} - 1)} \quad (3)$$

Substituting $I = 3$ kA, $\gamma_0 = 3$ into (3) we get $W_1'' \sim 2 \cdot 10^{16}$ eV/cm. The measured value of W_1 is $6 \cdot 10^{16}$ eV/cm, that is $W_1' \sim 4 \cdot 10^{16}$ eV/cm. Inserting $I = 3$ kA, $\kappa = 1,7$, $\gamma_0 = 3$ into Eq. (2) we get $(\overline{\theta_0^2})^{1/2} \sim 0.25$, this result being in good agreement with the estimate of the beam angular spread in the foil.

Let us now proceed to an explanation of the observed value of the critical magnetic field H_{crit} . As one can see, this quantity satisfies to the equilibrium condition $H^2/8\pi > \mathcal{P}$ with a great (10-15 times) overbalance, so it is improbable that H_{crit} is determined by this condition. Most likely, the $Q(H)$ dependence is a result of a decrease of the beam

angular spread in the diode, when passing to higher fields. As for the critical field, it corresponds to a situation when the diode angular spread becomes smaller than the foil scattering angle, so that the further increase of a magnetic field does not improve the angular characteristics of the beam.

An intense microwave radiation of the beam in the 10-40 HHZ range was registered. Preliminary study of the spectrum of this radiation performed by means of the cut-off waveguides and quasi-optical spectrometer showed that the spectrum depends on the magnetic field strength. The observed spectrum can be interpreted as that of a cyclotron radiation of relativistic electrons. However, the absolute intensity of this radiation is several orders of magnitude higher than the calculated one (for the beam with known density and angular spread). The source of this discrepancy may be the existence of the beam inhomogeneities with the scales smaller than a cyclotron radius of beam electrons r_H . Such inhomogeneities give rise to a coherent cyclotron radiation with the intensity of approximately $r_H^3 n_b \left(\frac{\Delta n_b}{n_b}\right)^2$ times higher than that of incoherent cyclotron radiation. Taking $n_b \sim 3 \cdot 10^{11} \text{ cm}^{-3}$, $r_H \sim 0,2 \text{ cm}$ we get that even for a very weak inhomogeneities ($\frac{\Delta n_b}{n_b} \sim 3 \cdot 10^{-4}$) the gain is about 300 times. The inhomogeneities may arise from the explosions of microspikes at the emitting surface of a cathode. We should note that these ideas of the mechanism of radiation are quite hypothetical and require the thorough experimental study.

4. Propagation of the Beam through a Plasma

As a rule, the propagation of the beam through a plasma was studied at the magnetic fields $H \geq 3 \text{ kOe}$. It was found out that the beam energy, measured with the exit calorimeter, depends noticeably on the density of a preliminary plasma. This fact was already pointed out in work [1], and also in our previous work [3], results of the last being shown in Fig. 4a.

One can see that in the density range $n = 10^{12} \div 10^{13} \text{ cm}^{-3}$ the beam loses 50-70% of its initial energy. At densities $n \geq 10^{13} \text{ cm}^{-3}$ the energy losses are considerably smaller and at $n \sim 10^{14} \text{ cm}^{-3}$ they become less than statistical scatter of the experimental data.

In the present run of experiments, with accelerator forced to give a higher current, the same measurements give a distinct result (Fig. 4b). Now, considerably more energy is transmitted through a dense plasma than through a vacuum. This is a result of injection of a supercritical current*). The amplitude of the exit current at densities $n \sim 10^{14} \text{ cm}^{-3}$ is equal to 5-5,5 kA - much greater than I_{crit} . The improvement of the beam transportation is due to the electric and magnetic neutralization of beam in a dense plasma.

By means of astralon plates it was determined that, when passing through the vacuum, the beam is quite symmetrical at the exit of machine, diameter of the beam being 2,5 cm (Fig 5a). If the beam passes through a plasma, it can be significantly

*) Note that in the experiments of Ref [3] injected current was close to the critical one.

deflected and simultaneously broadened (generally speaking, irregularly both in radial and azimuthal direction). In this regime the beam broadening is so strong that the beam can

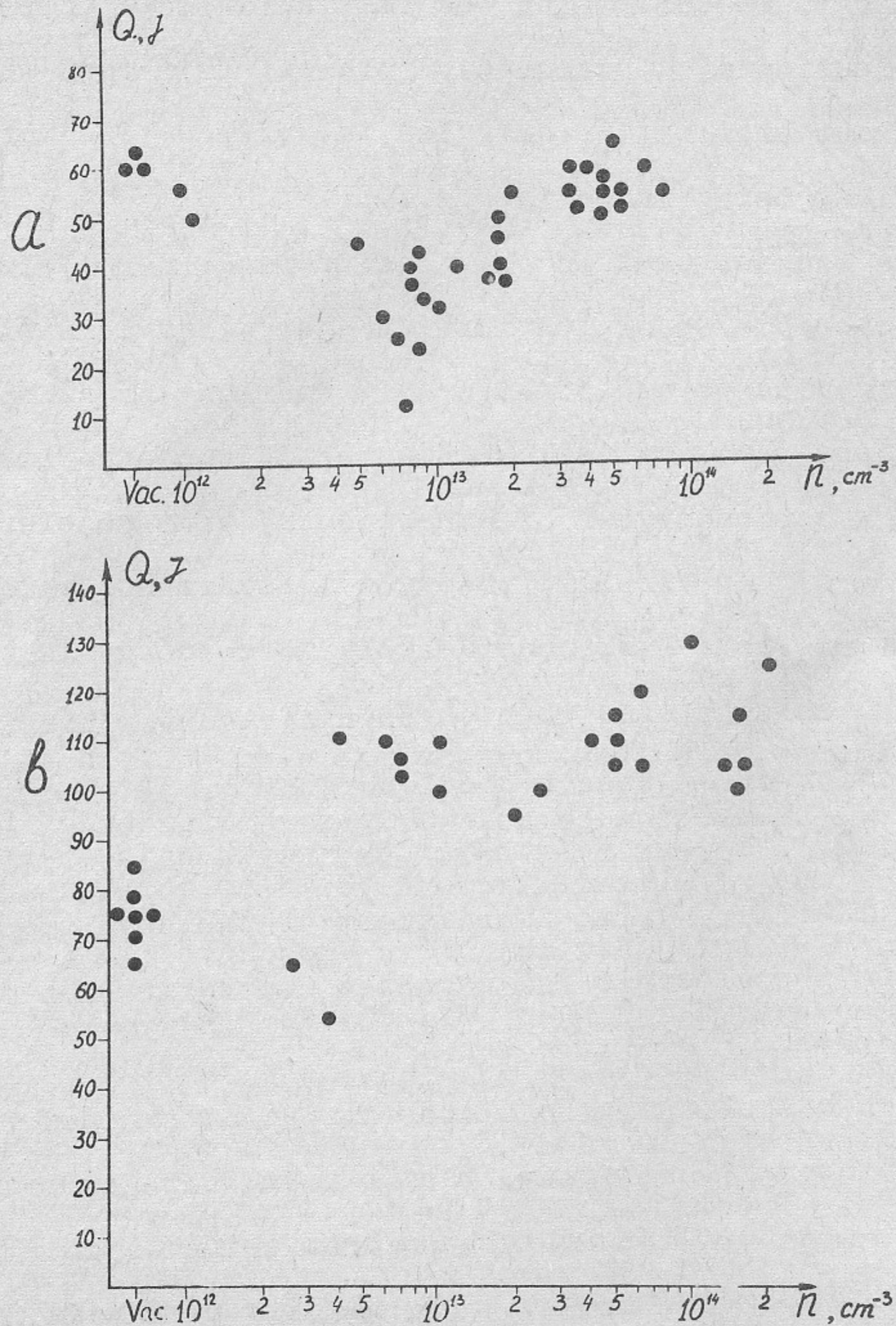


Fig.4. The transmitted beam energy as a function of the density of preliminary plasma, $H=7$ kOe.

be partially "eaten" by the walls of the vacuum chamber. If so, then the exit colorimeter will record high energy losses. Probably, such a behaviour of beam can be responsible for both the observed energy losses and their dependence on plasma density in experiments [1,3]. At high densities, broadening of the beam was small (Fig. 5c).

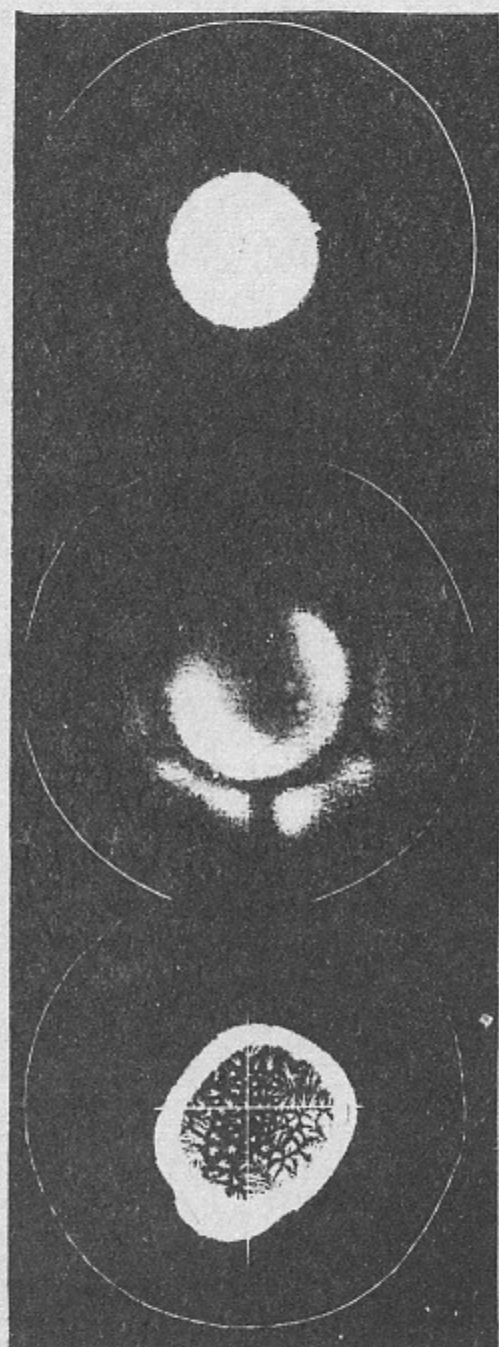


Fig.5. The shape of the beam cross-section: a-vacuum; b-plasma with density $n=2 \cdot 10^{12} \text{ cm}^{-3}$; c-plasma with density $n=5 \cdot 10^{13} \text{ cm}^{-3}$.

The observed behaviour of the beam can be explained by two effects: either by a macroscopic instability in $n < 3 \cdot 10^{13} \text{ cm}^{-3}$ density range, or by non-axisymmetrical distribution of the compensating plasma current with respect to a beam (which can arise due to inhomogeneities of the plasma conductivity).

Let us consider these two possibilities successively.

a spiral, winding on the return current. Due to this effect, the beam can be displaced at a distance 2Δ (see Fig.6) with respect to its initial position.

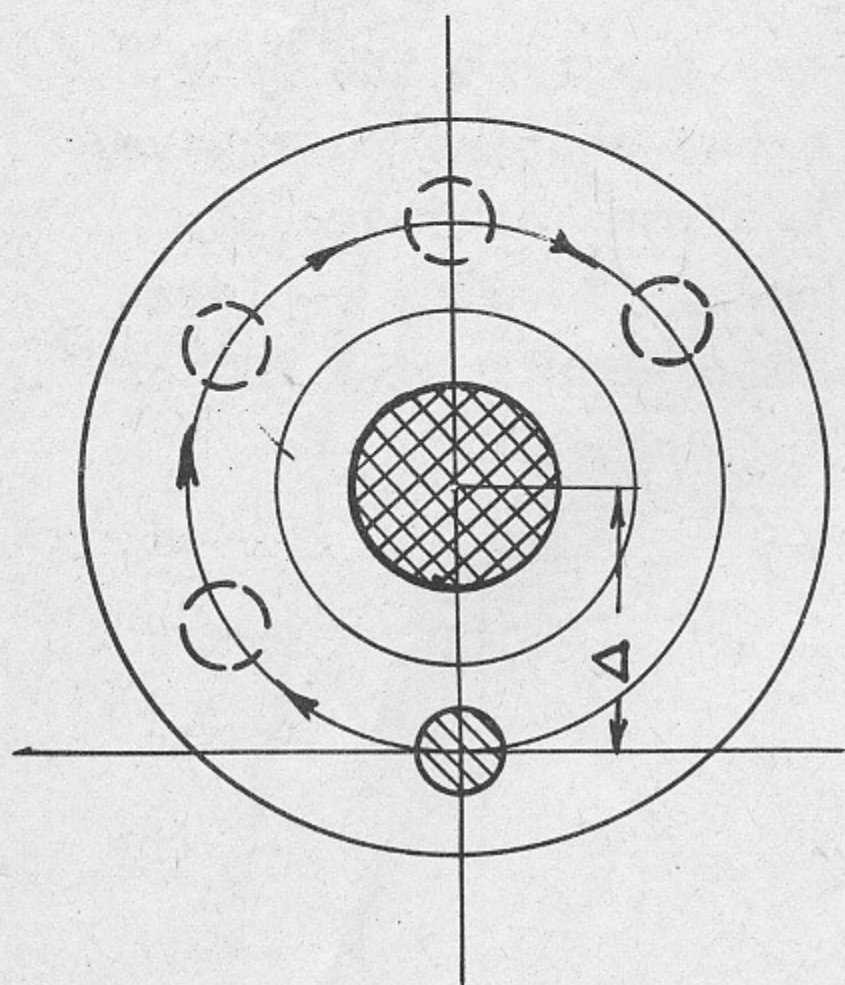


Fig.6 The influence of the inhomogeneities of plasma conductivity on the perpendicular displacements of the beam. The initial position of the beam is shaded. Double-shaded is the region of high conductivity. The circles are the magnetic field lines. Dashed circles are the positions of the beam at various distances from the entrance.

Owing to the changes in a beam current, the pitch of the spiral and, consequently, the position of the beam at the exit of machine, will depend on time. This means, that the beam will wander across the exit foil, and the time-integrated picture, obtained at the astralon plate, will show a rather smooth broadening of the beam.

The conductivity distribution is, of course, more smooth in experimental condition than in Fig.6, but this fact has no

Estimates show that in conditions of our experiment frequencies of the most important unstable oscillations lie in the range $\omega_{Hi} < \omega < \omega_{He}$, where ω_{Hi} and ω_{He} are the electron and ion gyrofrequencies, respectively. The unstable oscillations are of the helicon type, their dispersion being modified by the presence of beam. Calculation, which will be published elsewhere, show that the oscillations are localized in vicinity of the beam and have the growth rate $\text{Im}\omega \sim \frac{n_b}{n} \frac{c}{r_b}$

In order the instability to be effective, a condition $\tau \text{Im}\omega \geq 10$ (where τ is a beam duration) should be satisfied. Taking $r_b \sim 1,5 \text{ cm}$, $n_b \sim 3 \cdot 10^{11} \text{ cm}^{-3}$, $\tau \sim 5 \cdot 10^{-8} \text{ sec}$, one gets a following estimate for a marginal plasma concentration: $n_m \sim 3 \cdot 10^{13} \text{ cm}^{-3}$, instability being ineffective if $n > n_m$. This value of n_m does not contradict to experimental results: a noticeable spread of the beam exists at $n \leq 3 \cdot 10^{13} \text{ cm}^{-3}$.

The second possible explanation of the beam perpendicular broadening is connected with inhomogeneities of plasma conductivity. In the case of inhomogeneous conductivity, the plasma return current will be, generally speaking, displaced with respect to the beam axis, and the magnetic field of the return current will give rise to perpendicular wandering of the beam. The situation is illustrated with Fig.6, which corresponds to the case when the plasma conductivity is different from zero only in a narrow cylindrical region, displaced with respect to the beam axis. The return current creates a magnetic field with circular field lines. Under the joint action of this field and of the external one, the beam will move along

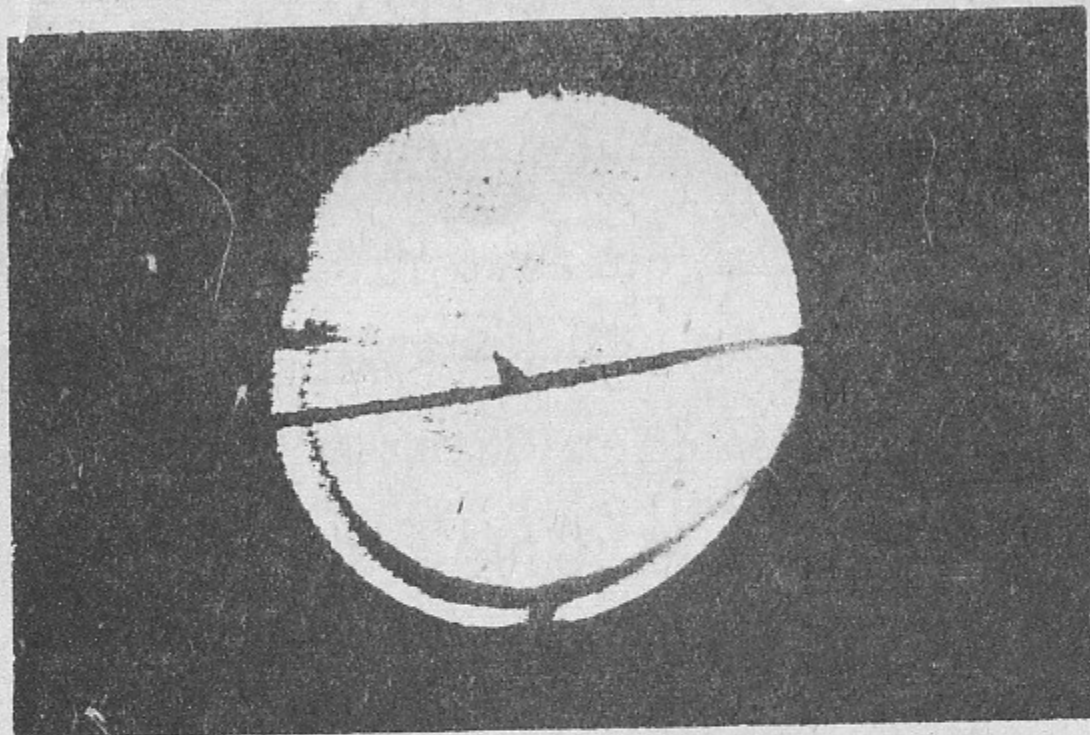


Fig.7. The picture of preliminary plasma cross-section, obtained with a plasmascope (plasma diameter 9cm, magnetic field 10 kOe, neutral hydrogen pressure $2 \cdot 10^{-3}$ torr).

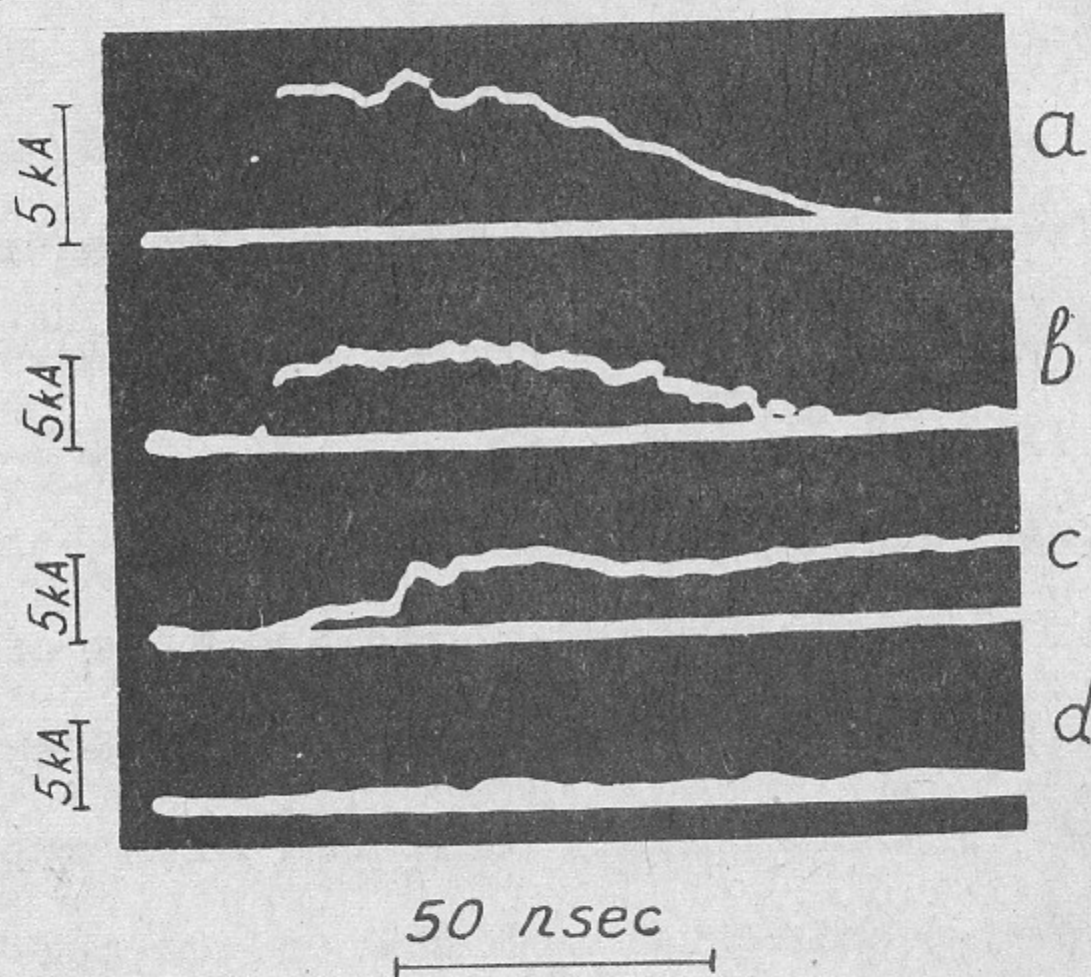


Fig.8 The typical oscillograms: a-exit beam current at $n \ 10^{14} \text{ cm}^{-3}$; b,c,d-total plasma current at densities 10^{12} cm^{-3} , 10^{13} cm^{-3} , and 10^{14} cm^{-3} , respectively; $H=7 \text{ kOe}$.

note

influence on the essence of the effect. One should only note that when the conductivity is very high, then its inhomogeneities do not play any role: the return current flows along the beam, and completely compensates the beam current, so that the beam displacement is absent.

The perpendicular distribution of the plasma density was studied by means of a plasmoscope which was placed instead of the exit foil. No significant density inhomogeneities were revealed (Fig.7). However, it is not yet clear, if the observed degree of homogeneity is sufficient to exclude the second of the explanations proposed.

Let us dwell now on the measurements of the total current in plasma. These measurements show that at plasma density $n \sim 10^{12} \text{ cm}^{-3}$ the beam current is not compensated (Fig.8b). At $n \sim 10^{13} \text{ cm}^{-3}$ the compensation is observed only at the forward front of the beam; at the backward front, the plasma current flows along the beam current, and then persists after decay of the beam (Fig.8c). At $n \sim 10^{14} \text{ cm}^{-3}$ the beam current is compensated at a very high degree (within 95% , Fig.8d), this being an evidence of a high conductivity of plasma.

5. Plasma Heating

beam

When the beam passes through a plasma, then diamagnetic signals become much longer and 5-7 times higher than in a vacuum case. The typical diamagnetic signals are shown in Fig.9. As a rule, the largest signal is observed at the first probe, signal at the second,

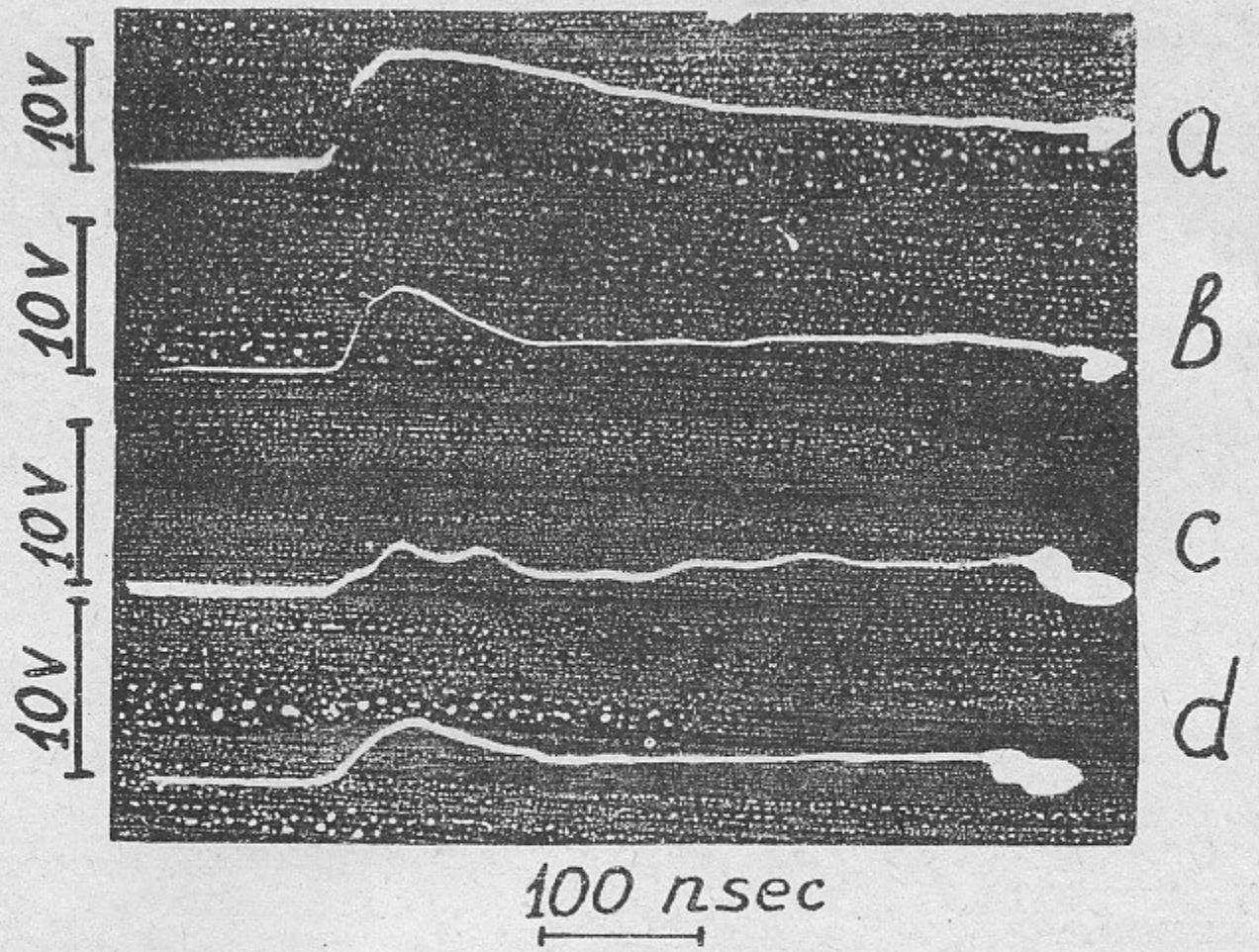


Fig.9 Typical signals from diamagnetic probes located at distances a-35cm, b-90cm, c-140cm, d-190cm from the entrance foil, respectively; $H=7$ kOe, $n=5 \cdot 10^{13}$ cm^{-3} .

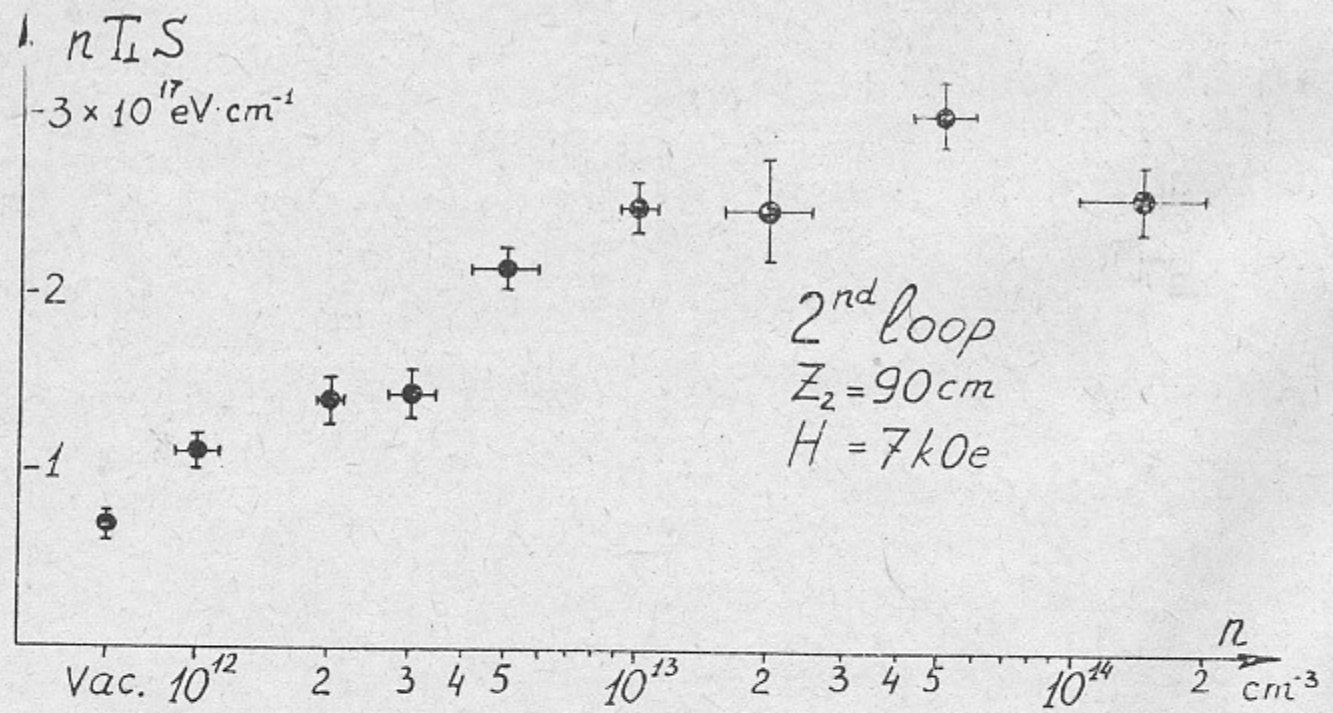


Fig.10 Dependence of plasma diamagnetism on the preliminary plasma density.

the third and the fourth probes being, respectively, 1,5, 2 and 3 times smaller. This fact shows that the reason of the observed diamagnetism is not the capture of beam electrons into the mirror machine. Otherwise, the diamagnetic signals would be equalized in a few nanoseconds (the flight time of relativistic electrons along the machine). Consequently, one can assume that the diamagnetism is due to plasma heating.

The dependence of the quantity $nT_1 S$ (which is the energy content per unit length of the plasma column) on the density of preliminary plasma is shown in Fig.10*). One can see, that diamagnetism grows monotonically up to densities $n \sim 5 \cdot 10^{13} - 10^{14} \text{ cm}^{-3}$. Note, that the density at which the diamagnetism reaches its maximum, is almost two orders of magnitude greater than that in the experiments of Ref. [1]. In our experiments, the maximum diamagnetism value is $nT_1 S \approx 3,5 \cdot 10^{17} \text{ eV/cm}$. If one assumes that the heating occurs only within the beam region ($S \approx 7 \text{ cm}^2$), then it follows from the previous data that $nT_1 \approx 5 \cdot 10^{16} \text{ eV/cm}^3$. At $n = 5 \cdot 10^{13} \text{ cm}^{-3}$ this corresponds to plasma temperature $T \approx 1 \text{ keV}$. The total energy content of the plasma column, as determined from diamagnetic measurements, is equal to 10-15 per cent of the beam energy.

*) The $nT_1 S$ values shown in Fig.10 are the maxima of diamagnetic signals at the second probe. Note, that the readings of the second probe with the reasonable accuracy correspond to the average value of diamagnetism along the plasma column.

After the beam passing through partly ionized plasma, an additional ionization was observed within ~ 500 nsec. Such an ionization could be produced by plasma electrons heated up to temperature ~ 1 keV. This value is in satisfactory agreement with temperature T_{\perp} obtained from diamagnetic measurements.

The dependence of diamagnetism on the external magnetic field strength is shown in Fig.11. At a given density, the diamagnetism grows monotonically with magnetic field.

One should note that, when passing to a dense plasma ($n \geq 10^{14} \text{ cm}^{-3}$), the character of diamagnetic signals is changed (see Fig.12). Regular oscillations appear now at the diamagnetic signals. These oscillations are especially pronounced at the second and at the third probes. The frequencies of these oscillations lie in the range 5-20 MHz, depending on the magnetic field strength and plasma density. The appearance of these oscillations is probably due to the excitation of magneto-acoustic oscillations, which is effective in the case when the heating time is shorter than the propagation time of a magneto-acoustic wave across the plasma. As one can see, this condition is well satisfied at densities $n \geq 10^{14} \text{ cm}^{-3}$ and magnetic fields $H \leq 3$ kOe.

Let us now consider the possible mechanisms of the observed plasma heating. In the density region $n \leq 10^{14} \text{ cm}^{-3}$ the pair collisions could be of importance only at low temperatures, $T < 20 \text{ eV}$, because at $T > 20$ eV the Coulomb collision time is longer than the beam pulse duration and the pair collisions can't be responsible for the observed heating of plasma to temperatures $T > 100$ eV.

In principle, the heating could be attributed to the

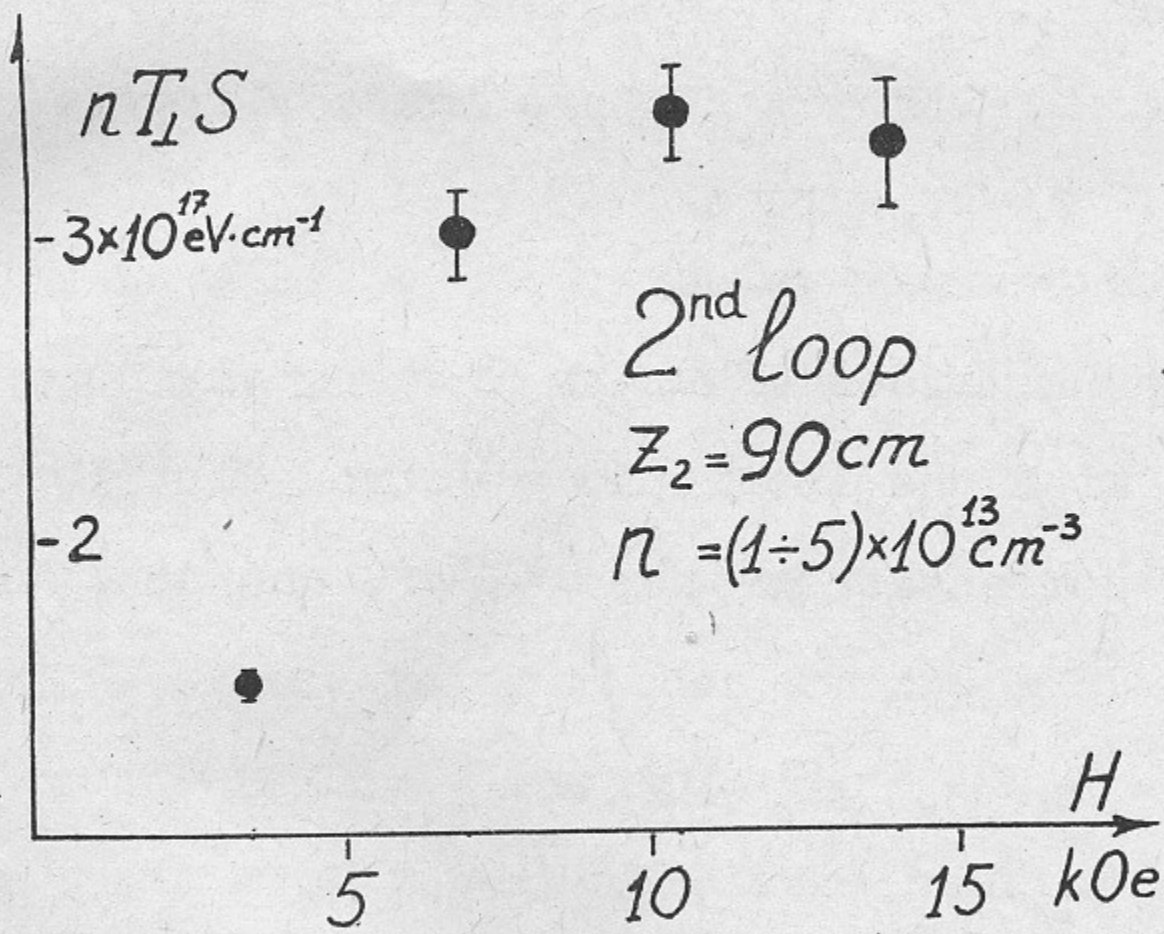


Fig.II The dependence of plasma diamagnetism on the magnetic field.

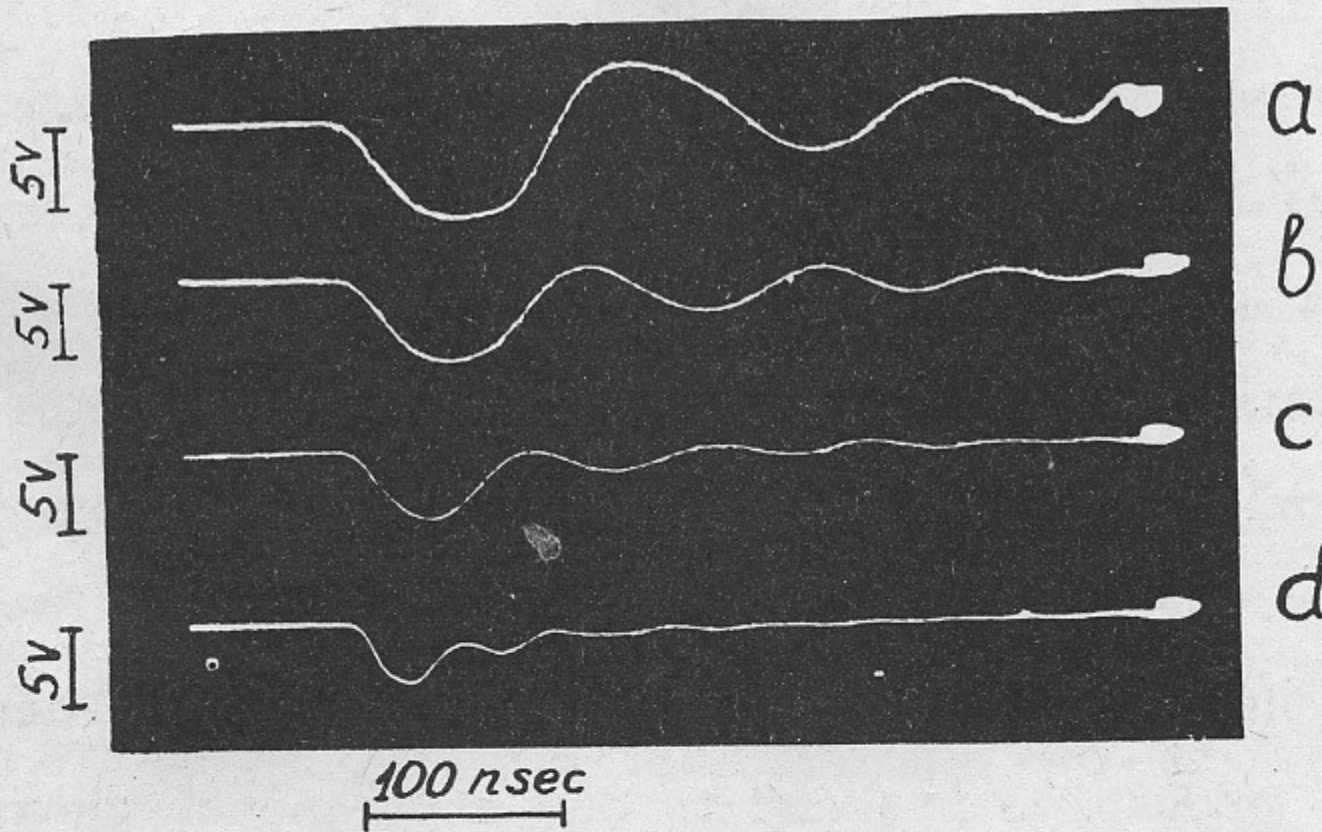


Fig.I2 Diamagnetic signals at the second probe ($z=90 \text{ cm}$) at high density of plasma ($n=2 \cdot 10^{14} \text{ cm}^{-3}$): a- $H=3.5 \text{ kOe}$, b- $H=7 \text{ kOe}$, c- $H=10 \text{ kOe}$, d- $H=14 \text{ kOe}$.

ion-acoustic instability excited by the return current. (This effect was first mentioned in Ref. [7], and later in Refs. [1,8]).

Indeed, the condition of excitation of this instability is

$$u > \alpha v_{Te} \sqrt{\frac{m}{M}}, \quad (4)$$

where v_{Te} is the electron thermal velocity and α is a numerical coefficient which is of the order of unity in strongly nonisothermal ($T_e \gg T_i$) plasma with the isotropic electron distribution.

If the beam current is compensated, then $u = \frac{n_b}{n} c$, and condition (4) takes the form:

$$\frac{n_b}{n} > \alpha \sqrt{\frac{m}{M}} \frac{v_{Te}}{c} \quad (5)$$

In our experiments, this inequality is always satisfied. However, the current compensation at $n \geq 3 \cdot 10^{13}$ is almost complete, that is, the excitation of the ion-acoustic instability*) does not limit the directed velocity of plasma electrons at the critical level (4), with $\alpha = 1$. The possible explanation of this phenomenon is the deformation of the electron distribution function in a longitudinal electric field, this deformation resulting in the increase of α up to the value $\sim \sqrt{M/m}$ (see [9, 10]).

It follows from the previous consideration that the ion-acoustic instability is, probably, present in our experiment. However, the simple electrotechnical estimates show that at least in the region of a good compensation, the contribution of the return

*) The condition $\tau \text{Im} \omega \geq 10$ is satisfied for the ion-acoustic instability with great overbalance: $\text{Im} \omega \approx \omega_{pi} \frac{u}{v_{Te}} = \omega_{pi} \frac{c}{v_{Te}} \frac{n_b}{n} \approx 5 \cdot 10^8 \text{ sec}^{-1}$ (for $n = 10^{14} \text{ cm}^{-3}$, $n_b = 3 \cdot 10^{11} \text{ cm}^{-3}$, $v_{Te} = 2 \cdot 10^9 \text{ cm/sec}$); $\tau = 5 \cdot 10^{-8} \text{ sec}$; $\tau \text{Im} \omega \approx 25$.

current into the plasma heating is insignificant. Indeed, the energy ΔQ dissipated in plasma by the return current I_r is

$$\Delta Q = \int_0^{\infty} I_r U_r dt,$$

where $U_r = \mathcal{L} \frac{d}{dt} (I_b - I_r)$ is the inductive voltage, and $\mathcal{L} = \frac{2L}{c^2} \ln \frac{R}{r_b}$ is the inductance of the system. One can show, that

$$\Delta Q \leq \mathcal{L} \max |I_b| \cdot \max |I_r - I_b|, \quad (6)$$

the inequality being rather strong. The oscillograms show that at $n \geq 5 \cdot 10^{13} \text{ cm}^{-3}$ $\max |I_r - I_b| < 0,05$. Then inequality (6) gives $\Delta Q \leq 2,5 \text{ J}$, that is plasma heating with return current is insignificant.

We think that the plasma heating (at least at $n > 3 \cdot 10^{13} \text{ cm}^{-3}$) can be attributed to the beam excitation of Langmuir oscillations. The corresponding instability has a high growth rate $\sim \frac{n_b}{n} \omega_{pe}$ and is characterized with the small scale of oscillations $\sim c/\omega_{pe}$ (see, for instance, [11, 12]). The calculations presented in Refs. [1, 2] show that in the conditions of our experiment the power liberated by the beam per unit volume of plasma is

$$q(z) \sim \frac{mc^3 n_b \gamma_0}{L^*} \frac{1}{\sqrt{\theta_0^2 + \frac{z}{L^*}}}$$

where z is a distance from the entrance foil and *)

$$L^* \sim \gamma_0^2 \frac{c}{\omega_{pe}} \left(\frac{mc^2}{T_e} \right)^2 \frac{8\pi n T_e}{H^2} \quad (7)$$

*) In contrast to paper [1] we do not write the factor T_i/T_e in formula (7). The necessity of this correction was marked in Ref. [13].

is a quantity which is called "relaxation length" (at distance L^* a beam liberates approximately the half of its initial energy).

The efficiency of plasma heating is:

$$\xi = \frac{\int_0^L q(z) dz}{mc^3 n_b \gamma_0} \approx \frac{L}{L^* \sqrt{\theta_0^2}} \quad (8)$$

Inserting into equations (7), (8) $n=10^{14} \text{ cm}^{-3}$, $T_e=10^3 \text{ eV}$, $H=7 \text{ kOe}$, $\theta_0^2=0.1$, one gets $\xi = 0.1$ in a reasonable agreement with the observations.

The effect of suppression of a beam instability by plasma inhomogeneities investigated in Ref. [14] was not important in our experiments due to high density of the beam.

Recently in paper [15] the mechanism of a beam relaxation was considered, based on the excitation of whistlers with short wave-lengths ($\lambda \sim c/\omega_{he}$). This mechanism turned to be very effective in some conditions. However, it can hardly play a significant role in our experiment, because the growth rate of whistler instability is small enough ($\text{Im } \omega \sim \omega_{he} \frac{n_b}{n}$), and group velocity of whistlers is rather high ($v_g \sim c \left(\frac{\omega_{he}}{\omega_{pe}} \right)^2$). As a result, whistlers cross the beam region in a very short time $\tau \sim r_b / v_g \ll (\text{Im } \omega)^{-1}$, and the whistler instability becomes ineffective.

6. Conclusion

In this section the most essential results of the work are summarized.

I. It was shown that there exists a collisionless heating of a dense plasma (density up to $2 \cdot 10^{14} \text{ cm}^{-3}$) by an intense relati-

vistic electron beam. The heating efficiency is 10-15 per cent in optimum conditions.

2. The ion-acoustic instability and the anomalous plasma resistivity do not have any considerable influence on the beam energy dissipation in the region of high plasma density ($n > 3 \cdot 10^{13} \text{ cm}^{-3}$). In this region the experimental results do not contradict the theory of beam relaxation at Langmuir oscillations, developed earlier.

3. Considerable broadening of the beam in the region of low plasma densities ($n < 10^{13} \text{ cm}^{-3}$) is revealed. This effect can be responsible both for the value of energy losses and for their dependence on plasma density observed in previous experiments [1,3].

The authors are indebted to G.I. Budker for his support of this work, and to B.N. Breizman, E.P. Kruglyakov, and V.M. Fedorov for useful discussion. The authors are also grateful to A.V. Arzhanikov, O.P. Sobolev, G.I. Shulzhenko for their assistance.

References

1. A.T. Altyntsev, B.N. Breizman, A.G. Es'kov, O.A. Zolotovskiy, V.I. Korteev, R.Kh. Kurtmullaev, V.L. Masalov, D.D. Ryutov, V.N. Semenov. Plasma Physics and Controlled Nuclear Fusion Research, v.2, p.309, Vienna, 1971.
2. B.N. Breizman, D.D. Ryutov, P.Z. Chebotaev. J.E.T.P., 62, 1409, 1972.
3. V.S. Koydan, V.M. Lagunov, V.N. Lukyanov, K.I. Mekler, O.P. Sobolev. Proc. of the 5-th Europ. Conf. on Plasma Physics and Controlled Nuclear Fusion Research, p.161, Grenoble, 1972.
4. B.P. Sannikov. Proc. of the Symp. on High-Current Electronics, p.22, Tomsk, 1973.
5. E.I. Dobrokhotov, A.V. Jharinov, I.N. Moskaev, D.P. Petrov. Nucl. Fusion, 9, 143, 1969.
6. L.S. Bogdankevich, A.A. Rukhadze. Uspekhi Fiz. Nauk, 103, 609, 1971.
7. L.I. Rudakov. J.E.T.P., 59, 2091, 1970.
8. R.V. Lovelace, R.N. Sudan. Phys. Rev. Lett., 27, 1256, 1971.
9. G.E. Vekstein, D.D. Ryutov, R.Z. Sagdeev. J.E.T.P., 60, 2142, 1971.
10. A.A. Vedenov, D.D. Ryutov. In "Problems of Plasma Theory", v.6., p.3, Moscow, 1972.
11. Ya.B. Fainberg, V.D. Shapiro, V.I. Shevchenko. J.E.T.P., 57, 966, 1969.
12. B.N. Breizman, D.D. Ryutov. J.E.T.P., 60, 408, 1971.
13. B.N. Breizman, V.E. Zakharov, S.L. Musher. J.E.T.P., 64, 1500, 1973.

14. B.N.Breizman, D.D.Ryutov. J.E.T.P. Letters, II, 606, 1970.
15. B.N.Breizman. Proc. of the 6-th Europ. Conf. on Plasma Physics and Controlled Nuclear Fusion Research, Moscow, 1973.

Ответственный за выпуск С.Н.Родионов
Подписано к печати 18/УП.73г. № МН08379
Усл. 1,7 печ.л., тираж 200 экз. Бесплатно
Заказ № 60

Отпечатано на ротапринтере в ИЯФ СО АН СССР